

## Circular Dichroism at the Edge: Large X-ray Natural CD in the 1s → 3d Pre-Edge Feature of 2[Co(en)<sub>3</sub>Cl<sub>3</sub>]·NaCl·6H<sub>2</sub>O

Brian Stewart,<sup>\*,†</sup> Robert D. Peacock,<sup>\*,‡</sup> Lucilla Alagna,<sup>§</sup> Tommaso Proserpi,<sup>\*,§</sup> Stefano Turchini,<sup>§</sup> José Goulon,<sup>||</sup> Andrei Rogalev,<sup>||</sup> and Chantal Goulon-Ginet<sup>⊥</sup>

Department of Chemistry and Chemical Engineering  
University of Paisley, Paisley PA1 2BE, UK  
Department of Chemistry, University of Glasgow  
Glasgow G12 8QQ, UK  
ICMAT-CNR, AdR di Roma, CP 10, I-00016  
Monterotondo Stazione, Italy  
European Synchrotron Radiation Facility, BP 220  
F-38043 Grenoble Cedex, France  
Faculté de Pharmacie, Université de Grenoble  
F-38706 La Tronche, France

Received June 18, 1999

We report the first measurements of X-ray natural circular dichroism (XNCD) in an isolated pre-edge transition of a transition metal complex. XNCD is a very recently developed technique<sup>1,2</sup> exploiting the availability of high degrees of circular polarization from a helical undulator X-ray source. CD, the differential absorption of left and right circularly polarized radiation, is an important technique for the study of chiral geometries and chirally discriminating interactions in biomolecules and asymmetric catalysts. We have recently extended the measurement of natural CD to the X-ray region for the first time,<sup>1</sup> reporting the XNCD spectrum at the Nd L<sub>2,3</sub>-edges in axial single crystals of the lanthanide complex Na<sub>3</sub>Nd(digly)<sub>3</sub>·2NaBF<sub>4</sub>·6H<sub>2</sub>O. A notable feature of that work was the identification of chiral multiple scattering paths responsible for CD in the photoelectron continuum absorption (near-edge structure). The [Co(en)<sub>3</sub>]<sup>3+</sup> ion has served as a paradigm in the development of the structural chemistry,<sup>3</sup> spectroscopy,<sup>4</sup> and theory<sup>5–8</sup> of chiral transition metal compounds. The occurrence of a well-resolved pre-edge (1s → 3d) feature some 18 eV to low energy of the Co K-edge made this system a natural choice for our extension of XNCD studies to the transition metals. Transition metal pre-edge features are commonly used as diagnostics of both oxidation state and coordination geometry in interpreting the X-ray spectra of metallobiosites and their model compounds.<sup>9</sup> The possibility of providing additional local (element-specific) chirality information is one of the important potential applications of XNCD.

The most noticeable feature of the present work (Figure 1) is

<sup>†</sup> University of Paisley.

<sup>‡</sup> University of Glasgow.

<sup>§</sup> ICMAT-CNR.

<sup>||</sup> European Synchrotron Radiation Facility.

<sup>⊥</sup> Université de Grenoble.

(1) Alagna, L.; Proserpi, T.; Turchini, S.; Goulon, J.; Rogalev, A.; Goulon-Ginet, C.; Natoli, C. R.; Peacock, R. D.; Stewart, B. *Phys. Rev. Lett.* **1998**, *80*, 4799–4802.

(2) Goulon, J.; Goulon-Ginet, C.; Rogalev, A.; Gotte, V.; Malgrange, C.; Brouder, C.; Natoli, C. R. *J. Chem. Phys.* **1998**, *108*, 6394–6403.

(3) (a) Saito, Y.; Nakatsu, K.; Shiro, M.; Kuroya, H. *Acta Crystallogr.* **1954**, *7*, 636. (b) Saito, Y.; Nakatsu, K.; Shiro, M.; Kuroya, H. *Acta Crystallogr.* **1955**, *8*, 729–730.

(4) (a) Mathieu, J.-P. *C. R. Acad. Sci.* **1953**, *236*, 2395–2397. (b) McCaffery, A. J.; Mason, S. F. *Mol. Phys.* **1963**, *6*, 359–371. (c) Peacock, R. D.; Stewart, B. *Coord. Chem. Rev.* **1982**, *46*, 129–157.

(5) Moffitt, W. J. *J. Chem. Phys.* **1956**, *25*, 1189–1198.

(6) Mason, S. F.; Seal, R. H. *Mol. Phys.* **1976**, *31*, 755–775.

(7) (a) Strickland, R. W.; Richardson, F. S. *Inorg. Chem.* **1973**, *12*, 1025–1036. (b) Richardson, F. S. *Chem. Rev.* **1979**, *79*, 17–38.

(8) Evans, R. S.; Schriener, A. F.; Hauser, P. J. *Inorg. Chem.* **1974**, *13*, 2185–2192.

(9) Westre, T. E.; Kennepohl, P.; DeWitt, J. G.; Hedman, B.; Hodgson, K. O.; Solomon, E. I. *J. Am. Chem. Soc.* **1997**, *119*, 6297–6314.

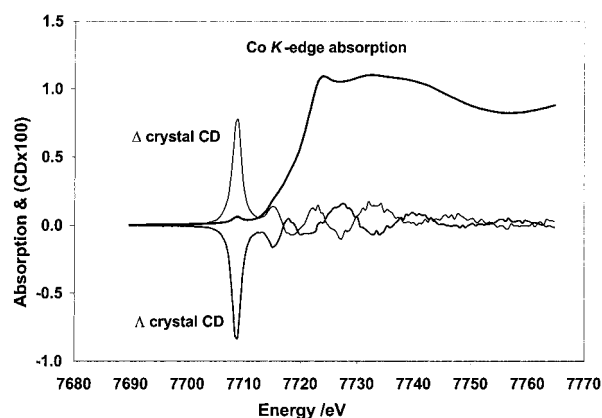


**Figure 1.** The Co K-edge absorption spectrum of an oriented single crystal of 2[Co(en)<sub>3</sub>Cl<sub>3</sub>]·NaCl·6H<sub>2</sub>O together with the XNCD spectra (multiplied by 100) of the  $\Lambda$  and  $\Delta$  enantiomers.<sup>10</sup>

the *spectacular size* of the 1s → 3d CD observed below the Co K edge. Measurements were made<sup>10</sup> with radiation propagating along the unique (3-fold) crystal axis. The Kuhn dissymmetry factor,  $g = (A_L - A_R)/(A_L + A_R)$ , is 12.5% if the raw CD and absorption are used. This magnitude is impossible to account for using the most common model of optical activity (the E1–M1 mechanism) which involves the interference between electric and magnetic dipole transition moments. We show below that an alternative mechanism (E1–E2), in which an electric dipole and an electric quadrupole interfere, is able to reproduce satisfactorily both the sign and magnitude of this effect. The E1–E2 mechanism was also found to be dominant in the XNCD of rare-earth L-edge XANES.<sup>1</sup>

For an isotropic sample, the contributions to the rotational strength are all of pseudoscalar symmetry, being formed from the interference (product) of transition tensors of the same rank but having opposite parity. The dominant contribution arises in most cases from the familiar electric dipole–magnetic dipole interference.

$$R_{ij} = \text{Im}\{ \langle i | \boldsymbol{\mu} | j \rangle \langle j | \mathbf{m} | i \rangle \}$$

In this case, the problem for core excitations is the selection rule forbidding a magnetic dipole transition moment for inter-shell,  $\Delta n \neq 0$ , transitions. In reality there is always relaxation of the core-hole state which removes the radial orthogonality between core and valence orbitals, providing a small magnetic dipole transition moment. While this mechanism is in principle effective for L-edge absorptions, magnetically allowing 2p → np, we have shown it to be insignificant for the rare-earth L-edges.<sup>1</sup> For the K-edge transitions the situation is worse still, requiring 1s–2p mixing in addition to the core relaxation effect. Hart *et al.* have measured the optical rotation of a powdered sample of [Co(en)<sub>3</sub>]-Br<sub>3</sub> through the Co K-edge and reported a significant ellipticity in the pre-edge region<sup>12</sup> but the interpretation of this measurement

(10) Crystals of 2[Co(en)<sub>3</sub>Cl<sub>3</sub>]·NaCl·6H<sub>2</sub>O were grown by slow evaporation from aqueous solution. Flat hexagonal plates with well-developed (111) faces were selected, and the unique (trigonal) axes were identified by polarized optical microscopy (observation of conoscopic figure) and confirmed by the appearance of the axial CD spectra and the absence of linear dichroism in the visible region. These procedures were necessary to avoid the possibility of X-ray artifacts due to linear dichroism and birefringence. Samples were cooled to a nominal 100 K and XNCD spectra obtained on the circularly polarized beamline (ID12A) at ESRF, Grenoble (France)<sup>11</sup> by monitoring the fluorescence at the Co K $\alpha$  line.

(11) Goulon, J.; Brookes, N. B.; Gauthier, C.; Goedkoop, J.; Goulon-Ginet, C.; Hagelstein, M.; Rogalev, A. *Physica B* **1995**, *209*, 199–202.

(12) Siddons, D. P.; Hart, M.; Amemiya, Y.; Hastings, J. B. *Phys. Rev. Lett.* **1990**, *64*, 1967–1970.

remains ambiguous due to the difficulties with the magnetic dipole mechanism mentioned above.

If oriented systems are considered, then the restriction to pseudoscalar quantities no longer holds and extra contributions to the rotational strength arise from product terms involving transition tensors of different rank. These contributions vanish for random orientation of the molecular system. The most important of them is the electric dipole–electric quadrupole contribution (E1–E2 mechanism) which, following the work of Chiu,<sup>13</sup> was elaborated by Buckingham and Dunn<sup>14</sup> and applied to the case of the visible d–d optical activity of oriented crystals containing the  $[\text{Co}(\text{en})_3]^{3+}$  ion by Barron.<sup>15</sup> Quadrupole-allowed transitions do not suffer from the inter-shell selection rule, and indeed there are a number of cases where quadrupole selection rules have been observed in isolated pre-edge features for transition metal K-edges.<sup>16</sup> These are good cases for the experimental measurement of X-ray CD since they are expected to possess high dissymmetry factors, being in a region of low background dipole strength.

For light propagating along the  $z$  axis in an oriented sample, such as a transition metal complex of  $D_3$  symmetry, the rotational strength in Cartesian components is given by<sup>17</sup>

$$R_{ij} = -(\omega_{ij}/c) \text{Re}\{\langle i|\mu_x|j\rangle\langle j|Q_{yz}|i\rangle - \langle i|\mu_y|j\rangle\langle j|Q_{xz}|i\rangle\} \quad (\text{E1-E2})$$

$$+ \text{Im}\{\langle i|\mu_x|j\rangle\langle j|m_x|i\rangle + \langle i|\mu_y|j\rangle\langle j|m_y|i\rangle\} \quad (\text{E1-M1})$$

The  $1s \rightarrow 3d$  transition is electric quadrupole-allowed and electric dipole- and magnetic dipole-forbidden in the octahedral parent symmetry and becomes partially electric dipole allowed in the  $C_3$  site symmetry of the complex in the crystal.

The present work extends the ab initio approach to the calculation of core-valence CD for the first time. To investigate the efficacy of the E1–E2 mechanism for the  $1s\text{--}3d$  transition, we have performed both frozen core and relaxed core HF calculations in a Gaussian orbital basis.<sup>18</sup> Such calculations of

the absorption spectra of transition metal complexes by ab initio methods are rare,<sup>19</sup> and there is only one example of an ab initio calculation of transition metal d–d NCD.<sup>20</sup> We used as our model complex the  $\Lambda\text{--}[\text{Co}(\text{en})_3]^{3+}$  ion in a  $D_3$  geometry optimization, starting from the crystal structure<sup>21</sup> of  $2[\Lambda\text{--Co}(\text{en})_3\text{Cl}_3]\cdot\text{NaCl}\cdot 6\text{H}_2\text{O}$ . As a check, the NCD of the magnetic dipole allowed  ${}^1A_1 \rightarrow {}^1A_2(T_{1g})$  and  ${}^1E(T_{1g})$  valence transitions were reproduced satisfactorily, with similar agreement to experiment to that found in refs 8 and 20. The results confirm the importance of the quadrupole–dipole interference term in the mechanism of the XNCD in this oriented crystal. The sign of the  $1s \rightarrow 3d$  pre-edge signal is correctly reproduced as is the order of magnitude of the Kuhn dissymmetry factor ( $g_{\text{calc}} = 0.11$ ,  $g_{\text{obs}} = 0.125$ ;  $R_{\text{calc}}(\text{E1} - \text{E2}) = -7.8 \times 10^{-44}$  cgsu,  $R_{\text{obs}} = -8.7 \times 10^{-44}$  cgsu). The source of electric dipole transition moment for the pre-edge CD is  $\sim 97\%$  Co-based, as expected for a transition emanating from the  $1s$  core orbital.

In regard to the large magnitude of the CD in the pre-edge excitation, it appears that the E1–E2 mechanism is particularly efficient in this system. The  $g$  factor for  $1s \rightarrow 3d$  is the same order of magnitude as that of the d–d excitations where the latter are dominated by the E1–M1 mechanism. As a comparison, the dissymmetry factor is approximately 22% for the  $3d \rightarrow 3d {}^1A_1 \rightarrow {}^1E(T_{1g})$  transition which is electric dipole- and magnetic dipole-allowed. The  $1s \rightarrow 3d$  transition is essentially pure quadrupole in character, with  $\sim 10\%$  electric dipole activity. Almost all of this borrowed transition moment is effective in the CD. The additional frequency factor in the E1–E2 mechanism provides a  $\sim 3000$ -fold enhancement compared to the same transition moments if they were operating in the visible spectral region.

Despite the expectation that XNCD would be a small effect, we have shown that it can readily be measured in the case of isolated, electric quadrupole-allowed pre-edge transitions in oriented systems. The sign of the XNCD can be correlated with the absolute configuration of the complex via the E1–E2 mechanism, providing an element specific probe of local chirality. Since current measurements can now detect  $g$  factors of order  $10^{-4}$ , this gives scope for the study of more dilute systems.

**Acknowledgment.** We thank the ESRF, the UK EPSRC, and the University of Paisley for support.

JA9920720

(19) Vanquickenborne, L. G.; Coussens, B.; Ceulmans, A.; Pierloot, K. *Inorg. Chem.* **1991**, *30*, 2978–2986.

(20) Ernst, M. C.; Royer, D. J. *Inorg. Chem.* **1993**, *32*, 1226–1232.

(21) We have redetermined the crystal structure of  $2[\Lambda\text{--Co}(\text{en})_3\text{Cl}_3]\cdot\text{NaCl}\cdot 6\text{H}_2\text{O}$ , Farrugia, L. J.; Peacock, R. D.; Stewart, B. *Acta Crystallogr., Sect. C*, submitted.

(22) Dykstra, C. E.; Augspurger, J. D. MAGOPS: one-electron operator program, Quantum Chemistry Program Exchange, program no. 585.

(23) Yokoyama, T.; Kosugi, N.; Kuroda, H. *Chem. Phys.* **1986**, *103*, 101–109; Kosugi, N.; Yokoyama, T.; Asakura, K.; Kuroda, H. *Chem. Phys.* **1984**, *91*, 249–256.

(24) Schirmer, J.; Braunstein, M.; McKoy, V. *Phys. Rev. A* **1990**, *41*, 283–300; Schmitt, A.; Schirmer, J. *Chem. Phys.* **1992**, *164*, 1–9.

(13) Chiu, Y. N. *J. Chem. Phys.* **1970**, *52*, 1042–1053.

(14) Buckingham, A. D.; Dunn, M. B. *J. Chem. Soc. (A)* **1971**, 1988–1991.

(15) Barron, L. D. *Mol. Phys.* **1971**, *21*, 241–246.

(16) Pickering, I. J.; George, G. N. *Inorg. Chem.* **1995**, *34*, 3142–3152.

(17) Barron, L. D. *Molecular Light Scattering and Optical Activity*; Cambridge University Press: Cambridge, 1982;  $\mu_x, \mu_y, m_x, m_y, Q_{xz}, Q_{yz}$  are components of, respectively, the electric dipole, magnetic dipole, and electric quadrupole operators.

(18) Scf eigenvectors produced by the GAMESS-UK program suite (Guest, M. F.; Sherwood, P., EPSRC Daresbury Laboratory, 1995) were used to construct the transition density matrices needed to evaluate all one-electron integrals<sup>22</sup> of the electric and magnetic dipole and electric quadrupole operators as well as the relaxed-frozen overlap integrals required for the relaxed core HF (RCHF) calculation. The computational methodology closely follows previous work on K-shell excitations in Cu(II) complexes<sup>23</sup> and the work of Schirmer et al<sup>24</sup> for the RCHF part. Using an extended basis set, scf convergences were carried out for the ground state and the K-shell ionised cation.